



Trace element and radiological characterisation of ash and soil at a legacy site in the former Raša coal-mining area

Tomislav Bituh¹, Josip Peco², Iva Božičević Mihalić³, Sabrina Gouasmia³, Marija Grlić⁴,
and Branko Petrincec^{1,5}

¹ Institute for Medical Research and Occupational Health, Division of Radiation Protection, Zagreb, Croatia

² University of Zagreb Faculty of Science, Department of Geology, Division of Mineralogy and Petrology, Zagreb, Croatia

³ Ruđer Bošković Institute, Laboratory for Ion Beam Interactions, Zagreb, Croatia

⁴ University of Zagreb Faculty of Science, Department of Biology, Zagreb, Croatia

⁵ Josip Juraj Strossmayer University of Osijek Faculty of Dental Medicine and Health, Osijek, Croatia

[Received in September 2024; Similarity Check in September 2024; Accepted in November 2024]

Coal mined in the shut-down Raša mine in Istria, Croatia had a high organic sulphur content. What has remained of its local combustion is a coal and ash waste (legacy site) whose trace element and radionuclide composition in soil has enduring consequences for the environment. The aim of this study was to follow up on previous research and investigate the potential impact on surrounding soil and local residents by characterising the site's ash and soil samples collected in two field campaigns. Trace elements were analysed using particle induced X-ray emission (PIXE) analysis. Radionuclides, namely ²³²Th, ²³⁸U, ²²⁶Ra, ²¹⁰Pb, and ⁴⁰K, were analysed with high resolution gamma-ray spectrometry. PIXE analysis confirms previous findings, whereas radionuclide analysis shows higher activity concentrations of ²³⁸U, ²²⁶Ra, and ²¹⁰Pb in ash samples than the worldwide average, and the absorbed dose rates for local residents are up to four times higher than background levels. Our findings confirm the need of investigating coal industry legacy sites and the importance of remediation of such sites.

KEY WORDS: ash; hazardous trace elements; NORM; PIXE; radionuclides; soil

LIST OF ABBREVIATIONS:

HR-ICP-MS – high-resolution inductively coupled plasma mass spectrometry; HTE – hazardous trace elements; IAEA – International Atomic Energy Agency; LOD – limit of detection; NORM – naturally occurring radioactive materials; PIXE – particle induced X-ray emission; PTE – potentially toxic elements; RBS – Rutherford backscattering spectrometry; SDD – silicon drift detector

The coal industry has been one of the leading polluting human activities due to its sizable emissions of hazardous particles and gases (1–4). Regardless of the environmental costs, many nations depend on coal as a major source of energy due to its great abundance and low price. However, coal is a “dirty fuel” in terms of human health (5). Depending on various geological factors, coal can contain hazardous trace elements (HTEs), such as Hg, As, Cr, Ni, V, Pb, Se, and Cd, and their levels are even higher in coal combustion by-products (6–8).

Another class of contaminants found in coal are naturally occurring radionuclides, formed either by incomplete fossil fuel combustion or coal formation. Coal contains trace quantities of uranium, thorium, and ⁴⁰K. According to the United Nations Scientific Committee on the Effects of Atomic Radiation

(UNSCEAR) (9), mean natural radionuclide concentrations in coal are 35 Bq/kg (range 16–110) for ²³⁸U, 35 Bq/kg (range 17–60) for ²²⁶Ra, 30 Bq/kg (range 11–64) for ²³²Th, and 400 Bq/kg (range 40–850) for ⁴⁰K.

Coal combustion by-products are fly ash (74 %), bottom ash (20 %), and boiler slag (6 %). Bottom ash consists of larger (heavier) particles collected at the bottom of the furnace. Fly ash is made of fine, airborne particles, most of whose content is recovered by stack emission control devices. The remainder is released into the atmosphere and later deposited on soil, contaminating it with HTEs (10–12) and radionuclides (13–21).

As the affected soils – particularly the ones of abandoned coal and ash waste sites – can be prone to erosion caused by winds and rain to release large amounts of coal and ash particles into the environment (8, 22), stringent environmental laws and efficient research and restoration strategies have been implemented to address these issues at legacy sites (23).

One such legacy site, Štrmac, is located near the town of Raša, which had the largest coal-mining company in Croatia in the 20th century, shut down since 1999 (24) (Figure 1). The site was used for the deposition of ash from the local foundries and heating plants, during which period they used domestic coal (anthracite from Istrian

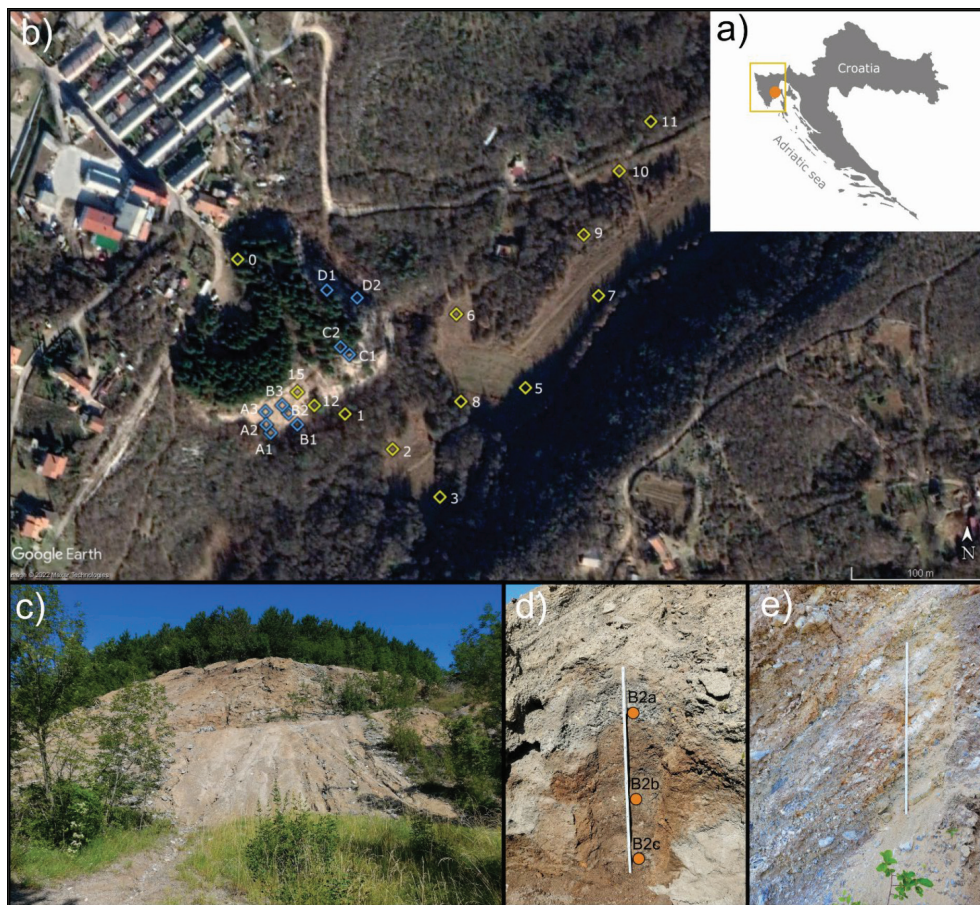


Figure 1 Overview of the research area. a) the geographical position of the Istrian Peninsula (North Adriatic Sea) and Štrmac settlement (orange circle); b) aerial view of the study area with marked sampling locations [yellow diamonds denote the first field campaign (May 2019) and blue diamonds the second (July 2019)]; c) the Štrmac coal burning waste disposal site; d) vertical B2 sampling profile with three subsamples – B2a, B2b, B2c; e) hill side with visible layers of progradation (the length of the vertical white line in d and e is 120 cm)

peninsula) with higher radionuclide amounts and higher radioactivity levels (25). Today, this legacy site is a 30-metre tall hill covered with vegetation (Figure 1c). The same coal was used by the Plomin coal-fired power plant but was never deposited at the site.

Previous environmental research (26–29) revealed the detrimental effects of coal combustion on all environmental compartments, mainly reflected in significantly increased levels of Se, V, and U in soil and biota. Moreover, Raša coal is known for its high content of organic sulphur (>14 %) (27, 28).

There are many coal fly ash legacy sites worldwide. However, measurements of radioactivity in fly ash at such sites are poorly reported. The reasons may be that most of the worldwide sites have been remediated or that most of the fly ash has been repurposed by construction industry. This, however, is not the case with the Štrmac site, and we believe it is important to characterise the site to obtain more information for possible solutions of remediation in the future.

The aim of our study was follow up on previous research by determining trace element and radionuclide levels at this legacy site and assess a potential impact on the surrounding soil and health of local residents.

METHODS

Study site and sampling

The Štrmac legacy site is situated on the Istrian peninsula to the NW of the former Adriatic carbonate platform (30) and is a part of the Outer Dinarides (31). In the late Carboniferous, the Adriatic platform was located in the north of Gondwana and subsequently formed a distinct carbonate platform in the early Jurassic only to disintegrate in the Cretaceous (32). Considering its paleogeology, the majority of the Istrian bedrock consists of carbonates, most of which are Mesozoic and early Cenozoic limestone. The Istrian peninsula consists of three distinct geological units: 1) the Jurassic-Cretaceous-Eocene carbonate plain in the south and west, 2) the Cretaceous-Eocene carbonate-clastic zone across the thrust structure in east and north-east, and 3) the Eocene flysch sediments in the central part (32).

The study site (Figure 1) is located in the Raša River basin containing deposits of bituminous Paleocene Kozina limestone (33, 34). The settlement of Štrmac is situated in the southeastern part of the Istrian peninsula on “terra rossa” cambic soil formed by insoluble residues of Eocene limestone with flysch sediments and

loess (30). It is close to the Plomin bay, which is a part of the northern Adriatic Sea (about 5 km of air distance).

Two field campaigns were carried out, in May and July 2019. In the first field campaign, ash and soil samples were collected from 13 locations in the Štrmac area, while in the second field campaign only ash samples were collected from 10 sampling locations (Table 1), with subsamples of different horizons along the vertical profiles (Figure 1d and 1e).

The sampling locations were chosen randomly, depending on accessibility, with the aim to investigate the potential influence of atmospheric events on the surrounding environment. Previous investigations at the site showed potential cytotoxicity of soil (33). Additionally, during sampling, we noticed private vegetable gardens in the vicinity, owned by the local community.

Soil and ash samples were air-dried, crushed, sieved through a 1 mm sieve, and homogenised in an agate mortar for further analysis.

PIXE elemental analysis

Particle induced X-ray emission (PIXE) elemental analysis was performed at the Ruđer Bošković Institute Tandem Accelerator Facility with 2 MeV proton beam obtained from 1 MV Tandetron accelerator (HVE Tandetron 4110, High Voltage Engineering Europa B.V., Amersfoort, Netherlands). The beam spot size on the sample was 3 mm in diameter. Emitted characteristic X-ray lines were measured simultaneously with two X-ray detectors, while backscattered ions were measured with a surface barrier detector using Rutherford backscattering spectrometry (RBS). For low-energy

Table 1 Sample labels and geographical coordinates

1 st field campaign (May 2019)				
Sample label	Sample type	Geographical coordinates		
0		45° 7' 14.40" N	14° 7' 36.86" E	
1		45° 7' 10.80" N	14° 7' 40.40" E	
2		45° 7' 9.98" N	14° 7' 41.97" E	
3		45° 7' 8.87" N	14° 7' 43.53" E	
5		45° 7' 11.41" N	14° 7' 46.35" E	
6	Soil	45° 7' 13.12" N	14° 7' 44.07" E	
7		45° 7' 13.55" N	14° 7' 48.76" E	
8		45° 7' 11.09" N	14° 7' 44.22" E	
9		45° 7' 14.97" N	14° 7' 48.27" E	
10		45° 7' 16.45" N	14° 7' 49.44" E	
11		45° 7' 17.60" N	14° 7' 50.48" E	
12				
13	Ash	45° 7' 10.88" N	14° 7' 39.14" E	
14				
15		45° 7' 11.31" N	14° 7' 38.83" E	
2 nd field campaign (July 2019)				
Sample	Subsample	Sample type	Geographical coordinates	
A1	A1		45° 7' 10.36" N	14° 7' 37.95" E
A2	A2a		45° 7' 10.55" N	14° 7' 37.80" E
	A2b			
A3	A3a		45° 7' 10.85" N	14° 7' 37.78" E
	A3b			
	A3c			
B1	B1a		45° 7' 10.55" N	14° 7' 38.83" E
	B1b			
B2	B2a	Ash	45° 7' 10.82" N	14° 7' 38.54" E
	B2b			
	B2c			
B3	B3a		45° 7' 11.00" N	14° 7' 38.33" E
	B3b			
C1	C1		45° 7' 12.18" N	14° 7' 40.54" E
C2	C2		45° 7' 12.36" N	14° 7' 40.25" E
D1	D1		45° 7' 13.68" N	14° 7' 39.80" E
D2	D2		45° 7' 13.50" N	14° 7' 40.80" E

X-rays we used a silicon drift detector (SDD) (Vitus H20, KETEK GmbH, Munich, Germany) with the active area of 10 mm² and 8 µm thick Be window. It is placed at the distance of 110 mm from the sample at an angle of 150 ° to the incident beam. For energies above 3.5 keV we used a Si(Li) detector (SSL80165, Canberra, Meriden, CT, USA) with 30 mm² active area and 25 µm thick Be window, positioned at the angle of 135 ° and covered with a Mylar filter (275 µm). For backscattered ions we used a surface-barrier detector (Ultra, Ortec, Oak Ridge, TN, USA), placed at the angle of 165 ° from the incident beam. The schematic of the standard chamber for PIXE/RBS experimental setup is shown in Figure 2.

The energy spectrum was determined using a multichannel analyser coupled with a homemade data acquisition system SPECTOR. Each sample was irradiated with 0.6 nA with a total charge of 0.6 µC. The PIXE experimental setup was calibrated with two standards: Standard Reference Material (SRM) 2710 Montana Soil and PTXRFIAEA08 Natural Soil, provided as a reference material from the International Atomic Energy Agency in 2014 (35). Samples were ground, and their powder pressed into pellets of 1 cm in diameter using a standard press with a pressure of 6.4 t/cm² and then mounted on the sample holder with carbon tape.

Proton backscattered spectra were analysed with the SIMNRA simulation software (SIMNRA 7.0, Max Planck Institute for Plasma Physics, Garching, Germany) as described elsewhere (36) to determine the concentrations of major low Z elements (Z<10). For quantitative analysis of the obtained PIXE spectra we used the

GUPIXWIN software (GUPIXWIN 2.2.0, University of Guelph, Guelph, ON, Canada) (37) with a fixed matrix solution approach on thick targets and input matrix composition taken from SIMNRA results.

The accuracy of PIXE analysis was checked using the Standard Reference Material (SRM) 2710 Montana Soil and PTXRFIAEA08 Natural Soil.

Radioactivity analysis

For radioactivity analyses, soil and ash samples were prepared as described elsewhere (38, 39). Briefly, the samples were sieved (maximum grain size of 2 mm), dried at 105 °C for three days, ashed at 400 °C, and packed in 200 mL sealed cylindrical containers.

Radionuclide activity in the obtained ash was determined from the activity of decay product with a shorter half-life ($T_{1/2}$) under the assumption of a secular equilibrium between radionuclides. In undisturbed soil, the secular equilibrium between ²³⁸U and ²³⁴Th and between ²³²Th and ²²⁸Ac was established naturally. However, the loss of gaseous ²²²Rn from the surface layer of soil and during sample preparation resulted in a disequilibrium between ²²⁶Ra and ²¹⁴Pb. In order to restore the equilibrium, sealed samples were left to rest for more than 30 days.

Radionuclide activity concentrations were measured using high-resolution gamma-ray spectrometer with a high-purity germanium coaxial detector (Ortec GMX, Oak Ridge, TN, USA) at relative

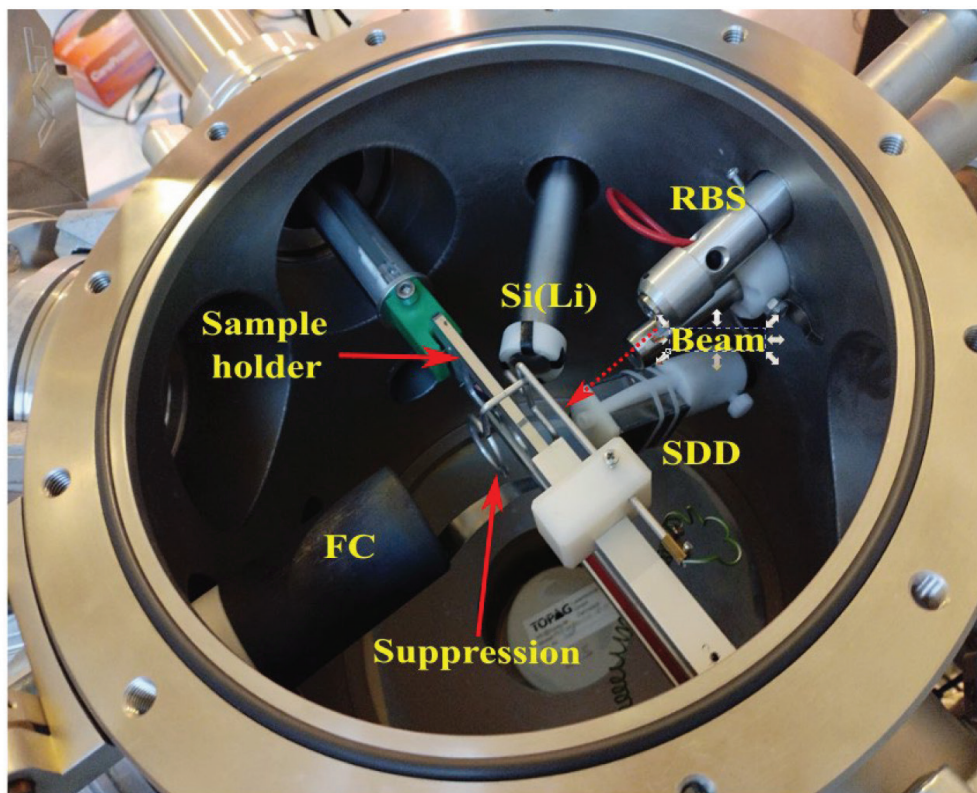


Figure 2 Standard IBA experimental chamber for PIXE and RBS measurements with marked positions of detectors, sample holder, suppression, Faraday cup, and incoming beam

efficiency of 74.3 % and energy resolution of 2.23 keV, all at ^{60}Co 1.33 MeV. The counting time was 80,000–250,000 seconds. Efficiency and energy were calibrated using certified standards (CBSS2 MIX, Eurostandard CZ, Czech Republic). The participating laboratory is accredited according to the ISO/IEC 17025 standard and the quality assurance was carried out by participation in proficiency testing provided by the IAEA and the European Commission's Joint Research Centre (40).

The detailed procedure for the analysis of soil samples, peak analysis, and self-attenuation corrections has been described in detail elsewhere (41–44). The typical values of the detection limit (for measurements of 80,000 s) were 1 Bq/kg for ^{232}Th and ^{226}Ra , 2 Bq/kg for ^{40}K , 3 Bq/kg for ^{210}Pb , and 4 Bq/kg for ^{238}U .

The radiological effects of the legacy site and the surrounding soil on the local population were assessed by calculating the radium equivalent index (Ra_{eq}), external absorbed dose rate (\dot{D}), and annual effective dose (E). The Ra_{eq} is used to define a uniform value with respect to radiation exposure in case the ash from the waste site were to be used as building material and is calculated using Equation 1.

$$Ra_{eq} = A_{Ra} + 1.43A_{Th} + 0.077A_K \quad [1]$$

where A_{Ra} , A_{Th} and A_K are the activity concentrations of ^{226}Ra , ^{232}Th and ^{40}K , respectively.

The weights were based on the estimation that 370 Bq/kg of ^{226}Ra , 259 Bq/kg of ^{232}Th , and 4810 Bq/kg of ^{40}K produce the same gamma-ray dose. If the Ra_{eq} values exceed the threshold value of 370 Bq/kg, the material will produce exposure higher than 1.5 mSv/year to local residents (45–47).

The UNSCEAR guidelines (9) provide the absorbed dose rates (\dot{D}) in nGy/h due to gamma radiation in air at 1 m above the ground for uniform distribution of naturally occurring radionuclides (^{226}Ra , ^{232}Th , and ^{40}K). The absorbed dose rates were calculated as follows:

$$\dot{D} = 0.462A_{Ra} + 0.621A_{Th} + 0.0417A_K \quad [2]$$

The annual effective dose (E) in mSv was also calculated according to the UNSCEAR guidelines (9):

$$E = \dot{D} (nGy \cdot h^{-1}) \times 8760(h \cdot yr^{-1}) \times 0.2 \times 0.7(Sv \cdot Gy^{-1}) \quad [3]$$

where 0.7 Sv/Gy is the conversion coefficient from the absorbed dose in air to the effective dose received by adults, while 0.2 is the outdoor occupancy factor assuming that adults spend 20 % of their time outdoors.

Statistical analysis

Correlation between trace elements and Bonferroni correction were run on the PAST statistical software (PAST version 4.17, University of Oslo, Norway) assuming the significance level of $P < 0.05$. For correlations between radionuclides ^{238}U , ^{235}U , ^{226}Ra , ^{232}Th , ^{40}K , and trace elements we used Spearman's rank correlation ran on IBM SPSS software (IBM SPSS Statistics for Windows,

version 23.0, Armonk, NY, USA) also assuming the significance level of $P < 0.05$.

RESULTS AND DISCUSSION

PIXE findings

Table 2 compares the values of major elements (given in %) and of minor and trace elements (given as mg/kg) measured in 12 soil samples with the SRM 2710 Montana Soil. Relative errors for most major elements are up to 10 %, while for some trace elements, errors are higher due to very low elemental concentrations that are around the PIXE limits of the detection.

Figure 3 shows typical PIXE spectra collected with the SDD detector optimised for low energy X-rays (Figure 3a) and Si(Li) detector for higher X-ray energy (Figure 3b).

Mean concentrations and standard deviations of major, minor, and trace elements of the 12 studied soil samples are listed in Tables 3–5. Table 3 shows the concentrations of major elements in percentages, while Tables 4 and 5 show concentrations of minor and trace elements as mg/kg. The last row of each table shows average limits of detection (LOD) for each element.

Earlier, Petrović (48) reported soil elemental composition at Štrmac measured with high-resolution mass spectrometry with inductively coupled plasma (HR-ICP-MS) (Tables 4 and 5). Only one soil sample was taken near our sampling location 1. The reported concentration ranges mostly correspond to ours, save for Cu, Sr, and Pb, which are higher (Table 5). Differences in Pb concentrations are probably owed to differences in the measurement methods employed, as sample preparation for ICP-MS involves dissolving samples in acids, which may render Pb and Rb extraction from the soil incomplete. Even so, this comparison confirms that our PIXE method is satisfactorily accurate.

Compared to the values from the literature for world soils (Table 6), our measurements show much higher levels for Ni, Cr, P, and S. Higher P levels apply only to samples 7–12. Pb, Zn, and Ni levels are also elevated in almost all samples, but to a lesser extent. Similar findings were reported by previous studies (26–29). Moreover, the concentration of Se is extremely elevated, but since these measurements are around the PIXE's LOD, it is difficult to draw definitive conclusions about soil contamination with Se at Štrmac. Previous measurement with ICP-MS (16, 26–29) clearly confirm that high Se levels are owed to its high content in Raša coal, which is also true for coal in general (49). According to the Geochemical Atlas of the Republic of Croatia (50), coastal Croatia has the highest concentrations of most potentially toxic elements (PTE) in Croatia and higher than the world/European average.

Spatial arrangement of S and V

S and V were chosen for spatial comparison because both elements are known to have elevated concentrations in Raša coal

Table 2 Comparison between measured and certified values for standard reference materials SRM 2710 and PTXRFIAEA08 Natural Soil*

Element	SRM 2710			Natural soil		
	Mean±SD	Certified value ± error	Relative error (%)	Mean ± SD	Certified value ± error	Relative error (%)
Mg	0.8±0.2	0.853±0.04	-6.3	-	-	-
Al	6.5±0.2	6.44±0.08	1.1	17.99±0.06	15.2±0.4	18.4
Si	27.0±0.3	29.0±0.2	-6.8	17.68±0.06	18.7±0.4	-5.4
S	0.26±0.01	0.240±0.006	8.1	0.109±0.05	0.071±0.004	54.5
K	2.03±0.04	2.1±0.1	-3.7	0.023±0.003	0.034±0.002	-33.1
Ca	1.12±0.02	1.25±0.03	-10.3	-	-	-
Fe	3.28±0.03	3.4±0.1	-3.1	8.82±0.03	9.0±0.3	-2.2
Na	9000±400	11400±600	-21.3	-	-	-
P	1400±200	1060±150	30.7	-	-	-
Ti	2670±60	2830±100	-5.7	9200±100	9410±380	-1.9
V	90±20	76.6±2.3	21.5	280±50	270±19	4.7
Cr	80±30	39	98.0	30±20	31±3	6.7
Mn	9700±200	10100±400	-4.1	180±30	174±13	2.8
Ni	21±2	14.3±1	49.2	-	-	-
Cu	3150±40	2950±130	6.7	50±10	36±3.4	48.1
Zn	7100±100	6952±91	1.6	40±10	69±6	-34.2
Ga	-	-	-	50±20	33±3	45.9
As	400±100	626±38	-27.6	-	-	-
Se	-	-	-	60±40	2.3±0.3	2354.1
Br	250±50	15±2	1524.0	-	-	-
Sr	-	-	-	30±30	4.6±0.6	562.3
Zr	-	-	-	200±50	266±18	-23.8
Ba	540±70	707±51	-23.5	-	-	-
Hg	140±80	33±2	316.2	-	-	-
Pb	6800±200	5532±80	22.1	-	-	-

* Concentrations of major elements (Mg, Al, Si, K, Ca, Fe) and S are given in percentage, of minor and trace elements in mg/kg, and data accuracy as relative error in percentage

Table 3 Major and minor element concentrations (in %) in measured soil samples with limits of detection (LOD) for each element

Soil samples	Mg	Al	Si	S	K	Ca	Fe
1	1.5±0.1	2.3±0.2	2.2±0.1	3.6±0.2	0.015±0.09	29±3	1.58±0.02
2	1.25±0.01	7.91±0.03	22.82±0.07	0.180±0.005	1.45±0.01	7.21±0.03	4.22±0.04
3	1.29±0.004	9.22±0.03	26±1	0.09±0.01	1.5±0.1	1.11±0.03	4.92±0.06
5	1.13±0.01	8.85±0.03	27.90±0.09	0.09±0.004	1.43±0.01	0.984±0.009	4.73±0.08
6	0.82±0.01	6.3±0.02	19.32±0.03	2.94±0.01	0.763±0.008	6.94±0.02	3.44±0.02
7	1.03±0.03	5.3±0.1	16±1	0.06±0.01	1.25±0.03	19.4±0.04	2.574±0.08
8	1.03±0.01	8.34±0.04	28.4±0.1	0.293±0.006	1.43±0.01	1.31±0.01	4.33±0.07
9	1±0.01	7.88±0.03	30.5±0.1	0.227±0.006	1.34±0.01	1.26±0.01	4.1±0.08
10	0.98±0.01	8.76±0.03	31.11±0.08	0.156±0.006	1.34±0.01	0.862±0.09	4.43±0.09
11	0.89±0.01	8.24±0.04	26.9±0.01	0.176±0.006	1.29±0.01	1.19±0.01	3.95±0.07
12	1.25±0.02	1.17±0.01	1.16±0.01	8.26±0.04	--	26.2±0.1	0.93±0.01
LOD	0.01	0.007	0.006	0.007	0.005	0.01	0.002

LOD – limit of detection

Table 4 Minor and trace element concentrations (in mg/kg) in measured soil samples with limits of detection (LOD) for each element and comparison with trace element concentrations obtained with HR-ICP-MS in one sample taken close to location 1 reported by Petrović (48)

Soil samples	Na	P	Cl	Ti	V	Cr	Mn	Co	Ni
1	--	--	--	1180±70	200±10	160±40	200±100	--	20±10
2	1600±100	600±60	140±30	4170±70	150±20	450±40	1490±60	--	140±10
3	2300±100	760±60	120±10	5030±80	150±20	300±100	1700±100	--	159±6
5	2600±100	740±60	150±30	5390±70	140±20	350±30	2170±70	170±30	144±9
6	2000±100	130±60	200±30	4510±70	210±20	320±40	1000±50	--	104±8
7	1230±40	400±100	160±60	2600±200	90±10	400±200	500±40	--	82±4
8	3300±100	1470±70	130±30	4850±70	200±20	380±30	1770±60	--	100±10
9	2400±100	890±70	230±30	4740±70	150±20	270±30	1340±60	--	126±8
10	4000±200	800±70	120±30	6070±80	140±20	570±40	1370±60	--	110±8
11	3800±200	1350±80	400±40	5810±80	120±20	380±30	2180±70	--	85±8
12	--	--	100±30	710±60	130±20	100±60	360±80	--	--
Petrović (48)	--	--	--	--	183	167	--	--	96.3
LOD	200	100	50	40	50	50	60	200	10

LOD – limit of detection

Table 5 Trace element concentrations (in mg/kg) in measured soil samples with limits of detection (LOD) for each element and comparison with trace element concentrations obtained with HR-ICP-MS in one sample taken close to location 1 reported by Petrović (48)

Soil Samples	Cu	Zn	As	Se	Br	Rb	Sr	Y	Pb
1	180±50	70±20	20±10	20±10	30±10	--	550±20	60±20	70±40
2	73±9	120±10	--	--	30±30	210±40	250±30	--	120±90
3	51±6	160±50	--	--	--	360±50	70±50	--	130±20
5	44±8	130±10	--	--	60±30	330±40	140±30	--	200±100
6	86±8	130±10	--	--	40±20	130±30	210±30	--	170±80
7	30±30	90±10	--	--	20±20	120±20	504±6	--	90±60
8	39±8	110±10	--	20±20	60±30	260±40	100±30	--	200±100
9	37±7	120±10	--	--	--	230±40	130±20	--	110±90
10	24±8	100±10	--	40±20	30±30	220±40	90±20	--	100±100
11	41±7	100±10	--	23±9	--	180±30	130±20	--	140±90
12	72±9	13±7	20±10	--	--	--	580±40	--	--
Petrović	37.8	120	14.8	21.8	--	--	128	--	48.2
LOD	10	20	20	30	40	50	30	20	90

LOD – limit of detection

and ash (27), and their elevated concentrations in soil samples indicate soil contamination originating from the landfill. Although the comparison shows a rather weak correlation between S and V, their distribution by locations above and below the median mostly coincides (Table 7). The exceptions are location 12, with concentration above the median for S and below the median for V, and location 3, with concentration below the median for S and above the median for V. Generally, locations further away from the landfill have lower concentrations of either element, with the exception of locations 3 for S and 12 for V. This suggests that the source of soil pollution with S and V in Štrmac is ash from the landfill, but this

connection is not unequivocal, as there are spatial variations in the distribution of elements.

Correlation and distribution of element levels

Previous research (26–28) showed positive and statistically significant ($p < 0.05$) Kendall-Tau correlation between S, Se, and V in Raša coal and Raša coal ash samples. In this study we determined a positive ($r > 0.5$) and statistically significant ($p < 0.05$) correlation between S and As ($r = 0.58$; $p = 0.013$), and a negative ($r < -0.5$) and a

Table 6 Measured elements in this study (mg/kg) compared to world soils and Croatian legislation

Element	This research (mg/kg)	Croatian legislation (51) (mg/kg)	World soils (52, 53) (mg/kg)	World soils (54) (mg/kg)	Topsoil Europe (54) (mg/kg)	Geochemical atlas (50) (mg/kg)
Al	11700–92200		80000			78500
As	20	30	5	6.83	11.6	18
Br	20*–60		10	10		
Ca	8620–290000		14000			13300
Cl	100–400		300	300		
Co	170*	60	10	11.3	10.4	18
Cr	100–570	120	80	59.5	94.8	121
Cu	24–180	120	25	38.9	17.3	35.5
Fe	9300–49200		35000			41800
K	150–10500		14000			12500
Mg	8900–15000		9000			6800
Mn	200–2180		530	488	524	1082
Na	1230–4000		10000			3400
Ni	20–159	75	20	29	37	74.6
P	130–1470		750			650
Pb	70*–200	150	17		32	48.7
Rb	120–360		65	68	87	
S	600–82600		800			
Se	20*–40		0.3	0.44		
Si	22000–311100		280000			
Sr	70–580		240		130	86
Ti	710–6070		4000	7038	6070	4300
V	90–200		90	129	68	148
Y	60		20	23	23	28
Zn	13*–160	200	70	267	68.1	108

* Levels below LOD. Values from the Geochemical Atlas of Croatia are given as medians for coastal Croatia

Table 7 Ranking of sampling locations by measured S and V levels (from highest to lowest)

Sampling location	S (%)	Sampling location	V (mg/kg)
12	8.26	6	210
1	3.6	1	200
6	2.94	8	200
8	0.293	2	150
9	0.227	3	150
2	0.18	9	150
11	0.176	5	140
10	0.156	10	140
3	0.09	12	130
5	0.09	11	120
7	0.06	7	90

Levels above the median are highlighted in boldface

statistically significant correlation between S and Al ($r=-0.587$; $p=0.012$) and S and Fe ($r=-0.514$ and $p=0.0278$).

The R value for the S-Se correlation is 0.0237 ($p=0.919$) and for S-V 0.443 ($p=0.0581$). We believe that the absence of significant correlation between S and Se is owed to the unreliability of the PIXE method in characterising Se in these samples. The S-V correlation is close to significance, and it is possible that the rounding of measurement figures had an influence on this outcome. However, the Bonferroni correction showed that only Al-Fe ($p=0.021$), Rb-Fe ($p=0.049$), and Na-Ti ($p=0.049$) correlations were statistically significant. This indicates that some of the other correlation coefficients could be falsely significant, probably due to heterogeneous composition of soil samples, and that the correlation between these elements is the most reliable.

Due to the limitations of the PIXE method, the levels of rare earth elements – Ce, Be, Sc, Ri, and Li – were not determined in this study. However, we did find a positive and statistically significant correlation between Al and Ti, Fe and Ni, and Fe and Mn. The Cu-Zn correlation was positive but not statistically significant ($r=0.112$;

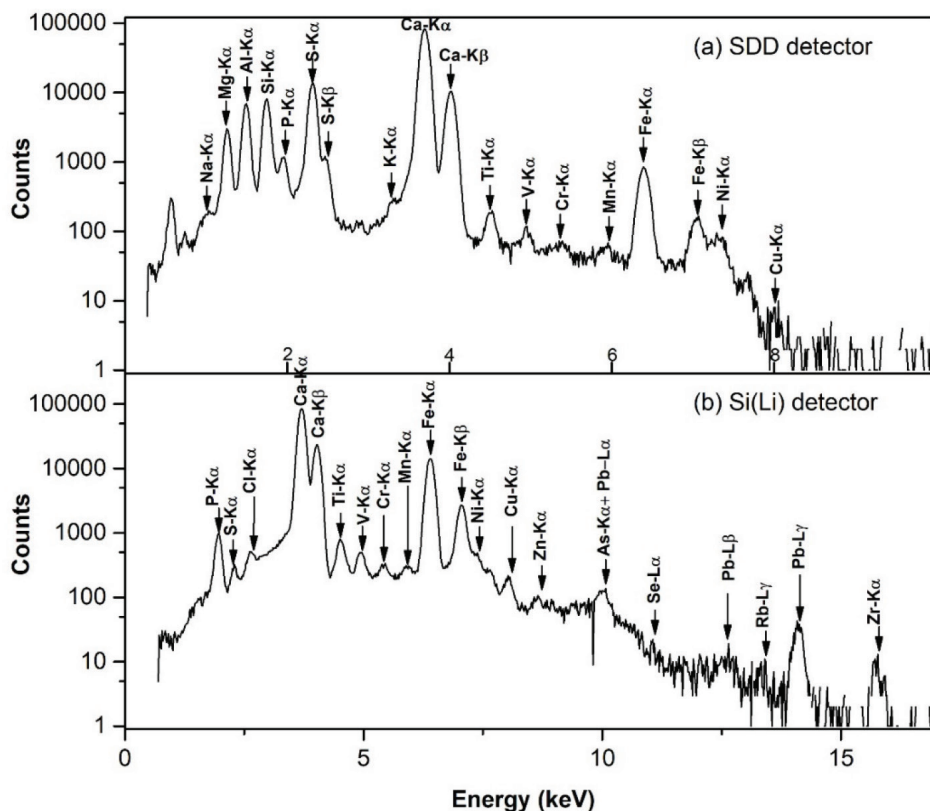


Figure 3 PIXE spectra of the soil sample taken with (a) SDD and (b) Si(Li) detector induced with 2 MeV protons

$p=0.631$). The results for the positive S-As correlation, which would normally indicate that As contamination at the landfill originated from Raša coal, are not reliable, as As was mostly below the detection limit. For the same reason, we found no correlations between Co and other elements.

Correlation between Al and Fe (Fe also correlates with Rb and K, Ni and Zn) stands out due to high correlation coefficients and small p-values ($r=0.927$, $p=7.18 \cdot 10^{-5}$). Considering the importance of Al, K, and Fe in the lithosphere and the formation of minerals, it is probably a natural correlation, but the additional correlation with Ni and Zn indicates a certain influence of the local foundry and/or heating plant in Štrmac.

Pollution indices

Pollution indices (PIs) are a simple way to assess the degree of pollution of soil, but they should be taken with reserve (55). The simplest of PIs, the single pollution index (SPI), is calculated by dividing a single heavy metal or PTE concentration in soil with “background geochemical values” or reference values such as those found in the Geochemical Atlas of Croatia (50). Other PIs for individual elements require additional data from different soil horizons or from a greater number of samples (56), which was out of our study’s scope.

If we apply pollution categorisation described by Kowalska et al. (56), the soil pollution at the Štrmac landfill is very strong for S,

Se, Co, and Cu (Table 8). This is in line with reports of high soil pollution indices in the wider area of Labin, including Štrmac for Hg, Cd, V, Se, Pb, Cr, Zn, Cu, U, and S (26–28), in which S had the highest and V the lowest index. Those indices were based on corresponding background levels reported in the Geochemical Atlas of Croatia (50). Our study shows a similar result regarding the relationship of S and V with other elements.

The lowest PIs are those calculated with the reference background levels taken from Croatian legislation for agricultural land (51). This legislation focuses on a small number of PTEs that the legislator considers relevant and sets their pollution limits. Even in these terms, the pollution is high for Cr and moderate for Cu and Ni. In contrast, the PIs for As, Pb, and Zn are below these limits for the soil to be considered polluted.

Radioactivity findings

Tables 9 and 10 show activity concentrations on naturally occurring radionuclides ^{232}Th , ^{238}U , ^{226}Ra , ^{210}Pb , and ^{40}K in soil and ash samples. Activity concentrations of ^{238}U , ^{226}Ra and ^{210}Pb were higher in ash samples, while ^{232}Th and ^{40}K activity concentrations were higher in soil samples. These results are in line with previous reports (9, 10, 19). Furthermore, the ranges of ^{232}Th , ^{238}U , ^{226}Ra , ^{210}Pb , and ^{40}K in soil samples (Table 10) are in good agreement with previous measurements of soil samples in this part of Croatia (43, 44).

Table 8 Pollution indices of selected elements in respect to reference values from Table 6 used in PI calculation*

Variables	Croatian ordinance (51)	World soils (52, 53)	World soils (54)	Topsoil Europe (54)	Geochemical atlas of Croatia (50)
As	0.67	4	2.93	1.72	1.11
Co	2.83	17	15.04	16.35	9.44
Cu	1.5	7.2	4.63	10.4	5.07
Cr	4.75	7.13	9.58	6.01	4.71
Fe		1.41			1.18
Mn		4.11	4.47	4.16	2.01
Ni	2.12	7.95	5.48	4.3	2.13
Pb	0.93	8.24		4.38	2.87
S		103.25			
Se		133.33	90.91		
Sr		2.42		4.46	6.74
V		2.22	1.55	2.94	1.35
Zn	0.8	2.29	0.6	2.35	1.48

* obtained by dividing the highest element level in the range with respective reference value

Table 9 Activity concentrations (Bq/kg) of natural radionuclides in soil and ash samples from Štrmac

	Sample code	Sample type	²³⁸ U	²³² Th	²²⁶ Ra	²¹⁰ Pb	⁴⁰ K
			Activity concentration ± relative uncertainty (Bq/kg)				
1 st field campaign	0	Soil	99±7	22±2	81±1	231±47	134±4
	2		58±6	44±2	44.1±0.9	52±47	433±10
	6		62±8	57±2	58.9±0.8	160±31	446±10
	7		50±4	20.8±0.9	23.2±0.6	171±33	354±9
	9		72±6	51±2	75±1	219±37	453±11
	11	138±9	67±3	81±1	238±37	464±12	
	14	Ash	458±10	17±2	349±3	288±29	302.6±0.9
	15		372±9	16±2	314±3	240±46	319±1
2 nd field campaign	A1	Ash	605±13	44±2	295±2	306±24	188±4
	A2a		567±10	34±2	440±2	318±20	183±6
	A2b		413±10	32±3	465±4	260±42	149±7
	A3a		440±15	42±3	551±3	341±31	173±7
	A3b		828±19	41±2	681±3	393±29	140±6
	A3c		401±12	29±2	376±2	303±24	162±7
	B1a		663±15	18±1	405±3	392±26	147±5
	B1b		306±8	16±1	341±2	227±27	147±6
	B2a		340±9	18±1	332±3	240±40	36±2
	B2b		308±8	13±1	316±2	168±31	137±8
	B2c		403±9	21±2	396±3	296±25	55±3
	B3a		304±7	7±1	326±2	230±37	141±6
	B3b		459±12	13±1	318±3	251±24	160±5
	C1		88±6	10±2	96±1	49±39	147±5
	C2		211±7	27±2	274±2	149±19	226±6
	D1		236±11	18±2	236±2	204±35	153±6
D2	250±7	9±1	225±2	193±33	118±5		

Table 11 summarises radium equivalent indices (Ra_{eq}), absorbed dose rates (D), and annual effective doses (E) in ash and soil calculated from activity concentrations of ^{226}Ra , ^{232}Th , and ^{40}K . The Ra_{eq} in most ash samples exceeded the threshold of 370 Bq/kg. Its wide range (122–751 Bq/kg) is probably owed to the inhomogeneity of the mined coal used for heating. To make use of this ash, it should be mixed it with other non-radioactive materials in ratios that comply with Croatian legislation (57).

The calculated absorbed dose rates originating from ash are higher than the background values for the Istrian region (70–80 nGy/h) (44), considering that the mean rate is 184 nGy/h, and the maximum is 346 nGy/h, about four times higher than the background rates.

The mean annual effective doses range from 0.05 mSv in soil to 0.42 mSv in ash. For comparison, the worldwide mean dose in soil is 0.07 mSv and ranges from 0.3 to 0.6 mSv across countries (9).

Spearman’s rank correlation shows positive ($r>0.9$) and statistically significant ($P<0.05$) correlation between radionuclides ^{238}U , ^{235}U , ^{226}Ra , ^{232}Th , ^{40}K and trace elements Na, P, and Ti. Only Sr correlated negatively ($r=-0.98$; $P=0.005$) with ^{238}U , ^{235}U , ^{226}Ra , and ^{40}K . We did not find any correlations between ^{210}Pb and any trace elements. However, due to a small number of soil samples, we cannot make solid conclusions on these correlations. In case of possible future remediation efforts, a more detailed investigation with a larger number of samples is required.

The future of the Štrmac legacy site is not known. Our findings, however, can inform remediation operations, should such decision be made. We already have positive precedents of remediation of coal fly ash deposition sites in Croatia (10, 58). Moreover, fly ash

can be used in construction industry. In European countries (France, Denmark, Italy, Germany, and the Netherlands) 85–100 % of produced coal fly ash is used for the production of cement, concrete, and ceramics (59, 60). There is also potential to extract rare earth elements, which are highly concentrated in coal fly ash, for use in batteries, lightweight alloys, and medical equipment, amongst several other applications, as reported elsewhere (61).

CONCLUSIONS

This characterisation of an abandoned ash dump in Štrmac (Labin locality, Croatia) provides important knowledge on the impact of trace elements and radionuclides on the environment and local community as it can help design better cleaning systems at combustion plants and improve deposition sites in the future.

Our findings show that all of the observed elements (Hg, Cd, V, Se, Pb, Cr, Zn, Cu, U, and S) highly contaminate soil. Furthermore, they confirm that the PIXE method is an acceptable supplemental non-destructive method for soil analysis, especially for highly concentrated elements such as sulphur, but cannot be used as the only research method.

High activity concentrations of ^{238}U , ^{226}Ra , and ^{210}Pb found in ash samples, radium equivalent indices exceeding the limit values, and the absorbed dose rates four times higher than background clearly highlight the need to remediate this legacy site.

We believe that our findings provide valuable information necessary for designing future deposition sites from the NORM industry and for remediating the current site or for using coal fly ash as raw material in the future.

Table 10 Mean, minimum, and maximum activity concentrations (Bq/kg) of natural radionuclides in soil and ash samples from Štrmac

Sample type		^{238}U	^{232}Th	^{226}Ra	^{210}Pb	^{40}K
		Activity concentration (Bq/kg)				
Soil	Average±SD	80±33	44±19	61±23	179±70	381±127
	Min	50	21	23	52	134
	Max	138	67	81	239	464
Ash	Average±SD	403±174	22±12	355±125	255±84	162±67
	Min	88	7	96	49	36
	Max	828	44	681	393	319

Table 11 Mean radium equivalent indices (Ra_{eq}), absorbed dose rates (D), and annual effective doses (E) in soil and ash samples at the Štrmac legacy site calculated from activity concentrations of activity concentration of ^{226}Ra , ^{232}Th , and ^{40}K

Sample type	Ra_{eq} (Bq/kg)	D (nGy/h)	E (mSv/year)
Ash (n=19)	399 (122–751)	184 (57–346)	0.23 (0.07–0.42)
Soil (n=6)	153 (80–213)	71 (38–99)	0.09 (0.05–0.12)

Ranges are given in parentheses

Acknowledgements

The authors would like to thank Dražen Vratarić, Dalibor Kvaternik, and Mladen Bajramović for help and advice related to the fieldwork, to Jasminka Senčar for gamma-ray spectrometry measurements, to Professor Damir Bucković for help with literature.

This work has partly been funded by the Division of Radiation Protection of the Institute for Medical Research and Occupational Health and the European Union – Next Generation EU programme project EBDIZ (Contract of 8 December 2023, Class: 643–02/23–01/00016, Reg. no. 533–03–23–0006). A part of the research was done at the facilities and with equipment funded by the European Regional Development Fund project KK.01.1.1.02.0007 “Research and Education Centre of Environmental Health and Radiation Protection – Reconstruction and Expansion of the Institute for Medical Research and Occupational Health”.

Conflict of interests

None to declare.

REFERENCES

- Finkelman RB, Wolfe A, Hendryx MS. The future environmental and health impacts of coal. *Energy Geoscience* 2021;2:99–112. doi: 10.1016/j.engeos.2020.11.001
- Boahen F, Száková J, Kališová A, Najmanová J, Tlustoš P. The assessment of the soil-plant-animal transport of the risk elements at the locations affected by brown coal mining. *Environ Sci Pollut Res* 2023;30:337–51. doi: 10.1007/s11356-022-22254-y
- Boaretto FBM, da Silva J, Scotti A, Torres JS, Garcia ALH, Rodrigues GZP, Gehlen G, Rodrigues VB, Charão MF, Soares GM, Dias JF, Picada JN. Comparative toxicity of coal and coal ash: Assessing biological impacts and potential mechanisms through *in vitro* and *in vivo* testing. *J Trace Elem Med Biol* 2024;81:127343. doi: 10.1016/j.jtemb.2023.127343
- Junior SFS, da Silva EO, Mannarino CF, Correia FV, Saggiaro EM. A comprehensive overview on solid waste leachate effects on terrestrial organisms. *Sci Total Environ* 2024;915:170083. doi: 10.1016/j.scitotenv.2024.170083
- Petrović M, Fiket Ž. Environmental damage caused by coal combustion residue disposal: A critical review of risk assessment methodologies. *Chemosphere* 2022;299:134410. doi: 10.1016/j.chemosphere.2022.134410
- Cheng W, Lei S, Bian Z, Zhao Y, Li Y, Gan Y. Geographic distribution of heavy metals and identification of their sources in soils near large, open-pit coal mines using positive matrix factorization. *J Hazard Mater* 2020;387:121666. doi: 10.1016/j.jhazmat.2019.121666
- Cao Q, Yang L, Ren W, Yan R, Wang Y, Liang C. Environmental geochemical maps of harmful trace elements in Chinese coalfields. *Sci Total Environ* 2021;799:149475. doi: 10.1016/j.scitotenv.2021.149475
- Petrović M, Ivanić M, Vdović N, Dolenc M, Čermelj B, Šket P, Medunić G, Fiket Ž. Physicochemical and mineral characteristics of soil materials developed naturally on two ~50 years old coal combustion residue disposal sites in Croatia. *Catena* 2023;231:107338. doi: 10.1016/j.catena.2023.107338
- UNSCEAR 2008 Report. Sources and Effects of Ionizing Radiation. Annex B – Exposures from natural radiation sources. New York: United Nations; 2010.
- Dragun Z, Stipaničev D, Fiket Ž, Lučić M, Udiković Kolić N, Puljko A, Repec S, Šoštarčić Vulić Z, Ivanković D, Barac F, Kiralj Z, Kralj T, Valić D. Yesterday's contamination – A problem of today? The case study of discontinued historical contamination of the Mrežnica River (Croatia). *Sci Total Environ* 2022;848:157775. doi: 10.1016/j.scitotenv.2022.157775
- Skoko B, Radić Brkanac S, Kuharić Ž, Jukić M, Štok M, Rovanić L, Zgorelec Ž, Perčin A, Prlić I. Does exposure to weathered coal ash with an enhanced content of uranium-series radionuclides affect flora? Changes in the physiological indicators of five referent plant species. *J Hazard Mater* 2023;441:129880. doi: 10.1016/j.jhazmat.2022.129880
- Zerizghi T, Guo Q, Wei R, Wang Z, Du C, Deng Y. Rare earth elements in soil around coal mining and utilization: Contamination, characteristics, and effect of soil physicochemical properties. *Environ Pollut* 2023;331:121788. doi: 10.1016/j.envpol.2023.121788
- Papastefanou C. Escaping radioactivity from coal-fired power plants (CPPs) due to coal burning and the associated hazards: A review. *J Environ Radioact* 2010;101:191–200. doi: 10.1016/j.jenvrad.2009.11.006
- Dinis ML, Fiúza A, Góis J, Carvalho JMS, Castro ACM. Modeling radionuclides dispersion and deposition downwind of a Coal-fired power plant. *Proced Earth Plan Sc* 2014;8:59–63. doi: 10.1016/j.proeps.2014.05.013
- Zhang W, Mo Q, Huang Z, Sabar MA, Medunić G, Ivošević T, He H, Urynowicz M, Liu FJ, Guo H, Haider R, Ali MI, Jamal A. Contaminants from a former Croatian coal sludge dictate the structure of microbiota in the estuarine (Raša Bay) sediment and soil. *Front Microbiol* 2023;14:1126612. doi: 10.3389/fmicb.2023.1126612
- Narayan A, Diogo BS, Mansilha C, Espinha Marques J, Flores D, Antunes SC. Assessment of ecotoxicological effects of Fojo coal mine waste elutriate in aquatic species (Douro Coalfield, North Portugal). *Front Toxicol* 2024;6:1334169. doi: 10.3389/ftox.2024.1334169
- Tyszka R, Pędziwiatr A, Pietranik A, Kierczak J, Ettl V, Mihačević M, Zieliński G. A long-term perspective on coal combustion solid waste interacting with urban soil. *Appl Geochem* 2024;166:105975. doi: 10.1016/j.apgeochem.2024.105975
- Marović G, Senčar J. Assessment of radioecological situation of a site contaminated by technologically enhanced natural radioactivity in Croatia. *J Radioanal Nucl Chem* 1999;241:569–74. doi: 10.1007/BF02347214
- Marović G, Senčar J, Bronzović M, Franić Z, Kovač J. Otpad vezan uz proizvodnju električne energije i proizvodnju mineralnih gnojiva [Radioactive waste due to electric power and mineral fertiliser production, in Croatian]. *Arh Hig Rada Toksikol* 2006;57:333–8.
- Habib MA, Khan R, Phoungthong K. Evaluation of environmental radioactivity in soils around a coal burning power plant and a coal mining area in Barapukuria, Bangladesh: Radiological risks assessment. *Chem Geol* 2022;600:120865. doi: 10.1016/j.chemgeo.2022.120865
- Gajbhiye T, Malik TG, Kang CH, Kim KH, Pandey SK. Assessment of sources and pollution level of airborne toxic metals through foliar dust in an urban roadside environment. *Asian J Atmos Environ* 2022;16:2021121. doi: 10.5572/ajae.2021.121

22. Petrović M, Fiket Ž, Medunić G, Chakravarty S. Mobility of metals and metalloids from SHOS coal ash and slag deposit: mineralogical and geochemical constraints. *Environ Sci Pollut Res* 2022;29:46916–28. doi: 10.1007/s11356-022-19074-5
23. Abdulmannan R, Skousen J, Tack FMG. An overview of soil pollution and remediation strategies in coal mining regions. *Minerals* 2023;13(8):1064. doi: 10.3390/min13081064
24. Buterin T, Doričić R, Broznić D, Čorić T, Muzar A. The Labin Region, an ecologically vulnerable geographical area in Croatia: Mortality characteristics in an area polluted by industrial over a 40-year period. *Geospatial Health* 2022;17:1082. doi: 10.4081/gh.2022.1082
25. Marović G, Senčar J, Kováč J, Prlić I. Improvement of the radiological environmental situation due to remedial actions at a coal-fired power plant. *J Radioanal Nucl Chem* 2004;261:451–5. doi: 10.1023/B:JRNC.0000034884.26071.a9
26. Medunić G, Singh PK, Singh AL, Rai A, Rai S, Jaiswal MK, Obrenović Z, Petković Z, Janeš M. Use of bacteria and synthetic zeolites in remediation of soil and water polluted with superhigh-organic-sulfur Raša coal (Raša Bay, North Adriatic, Croatia). *Water* 2019;11(7):1419. doi: 10.3390/w11071419
27. Medunić G, Bucković D, Prevendar Crnić A, Gaurina Srček V, Radošević K, Bajramović M, Zgorelec Ž. Sulfur, metal(loid)s, radioactivity, and cytotoxicity in abandoned karstic raša coal-mine discharges (the north Adriatic Sea). *Rud-geol-naft zb* 2020;35(3):50. doi: 10.17794/rgn.2020.3.1
28. Medunić G, Bilandžić N, Sedak M, Fiket Ž, Prevendar Crnić A, Geng V. Elevated selenium levels in vegetables, fruits, and wild plants affected by the Raša coal mine water chemistry. *Rud-geol-naft zb* 2021;36(1):52. doi: 10.17794/rgn.2021.1.1
29. Prevendar Crnić A, Damijanić D, Bilandžić N, Bilandžić N, Sedak M, Medunić G. Enhanced levels of hazardous trace elements (Cd, Cu, Pb, Se, Zn) in bird tissues in the context of environmental pollution by Raša coal. *Rud-geol-naft zb* 2022;37(1):57. doi: 10.17794/rgn.2022.1.3
30. Durn G, Ottner F, Slovenec D. Mineralogical and geochemical indicators of the polygenetic nature of terra rossa in Istria, Croatia. *Geoderma* 1999;91:125–50. doi: 10.1016/S0016-7061(98)00130-X
31. Malvić T, Velić J, Cvetković M, Vekić M, Šapina M. Definition of new Pliocene, Pleistocene and Holocene Lithostratigraphic Units in The Croatian part of the Adriatic Sea (Shallow Offshore). *Geoadrija* 2015;20:85–108. doi: 10.15291/geoadrija.2
32. Velić I, Tišljarić J, Vlahović I, Matičec D, Bergant S. Evolution of Istrian part of the Adriatic Carbonate Platform from the Middle Jurassic to the Santonian and formation of the flysch basin during the Eocene: Main events and regional comparison. In: Vlahović I, Tišljarić J, editors. *Field trip guidebook: evolution of depositional environments from the Palaeozoic to the quaternary in the Karst Dinarides and the Pannonian Basin*. Zagreb: Croatian Geological Survey; 2003. p. 3–18.
33. Medunić G, Ahel M, Božičević Mihalčić I, Gaurina Srček V, Kopjar N, Fiket Ž, Bituh T, Mikac I. Toxic airborne S, PAH, and trace element legacy of the superhigh-organic-sulphur Raša coal combustion: Cytotoxicity and genotoxicity assessment of soil and ash. *Sci Total Environ* 2016;566–567:306–19. doi: 10.1016/j.scitotenv.2016.05.096
34. Kuhta M, Brkić Ž. Seawater intrusion at abandoned coal mines in the Labin Region, Croatia. In: Goodwill J, editor. *Proceedings of the Third Annual International Conference on Mine Water Solutions*. Vancouver: University of British Columbia; 2018. p. 747–58.
35. International Atomic Energy Agency (IAEA). *Worldwide Open Proficiency Test for X ray Fluorescence Laboratories PTXRFIAEA08: Determination of Minor and Trace Elements in Natural Soil*. IAEA Analytical Quality in Nuclear Applications Series No. 38. Vienna: IAEA; 2014.
36. Mayer M. *SIMNRA User's Guide*. Report IPP 9/113. Garching: Max-Planck-Institut für Plasmaphysik; 1997.
37. Campbell JL, Boyd NI, Grassi N, Bonnicksen P, Maxwell JA. The Guelph PIXE software package IV. *Nucl Instrum Meth B* 2010;268:3356–63. doi: 10.1016/j.nimb.2010.07.012
38. International Atomic Energy Agency (IAEA). *Measurement of Radionuclides in Food and the Environment. A Guidebook*. Technical Reports Series No. 295. Vienna: IAEA; 1989.
39. International Atomic Energy Agency (IAEA). *IAEA-TECDOC-1415. Soil Sampling for Environmental Contaminants*. Vienna: IAEA; 2004.
40. Franić Z, Bituh T, Godec R, Čačković M, Meštrović T, Šiško J. Experiences with the accreditation of the Institute for Medical Research and Occupational Health, Zagreb, Croatia. *Arh Hig Rada Toksikol* 2020;71:312–9. doi: 10.2478/aiht-2020-71-3449
41. Vidmar T. EFFTRAN – A Monte Carlo efficiency transfer code for gamma-ray spectrometry. *Nucl Instrum Meth A* 2005;550:603–8. doi: 10.1016/j.nima.2005.05.055
42. Šoštarić M, Babić D, Petrinc B, Zgorelec Ž. Determination of gamma-ray self-attenuation correction in environmental samples by combining transmission measurements and Monte Carlo simulations. *Appl Radiat Isot* 2016;113:110–6. doi: 10.1016/j.apradiso.2016.04.012
43. Šoštarić M, Petrinc B, Avdić M, Petroci Lj, Kovarić M, Zgorelec Ž, Skoko B, Bituh T, Senčar J, Branica G, Franić Z, Franulović I, Rašeta D, Bešlić I, Babić D. Radioactivity of soil in Croatia I: Naturally occurring decay chains. *Arh Hig Rada Toksikol* 2021;72:6–14. doi: 10.2478/aiht-2021-72-3439
44. Šoštarić M, Petrinc B, Avdić M, Petroci Lj, Kovarić M, Zgorelec Ž, Skoko B, Bituh T, Senčar J, Branica G, Franić Z, Franulović I, Rašeta D, Bešlić I, Babić D. Radioactivity of soil in Croatia II: ¹³⁷Cs, ⁴⁰K, and absorbed dose rate. *Arh Hig Rada Toksikol* 2021;72:15–22. doi: 10.2478/aiht-2021-72-3440
45. United Nations Scientific Committee on the Effects of Atomic Radiation (UNSCEAR). *Ionizing Radiation: Sources and Biological Effects*. New York: UNSCEAR; 1982.
46. Farai IP, Ademola JA. Radium equivalent activity concentrations in concrete building blocks in eight cities in Southwestern Nigeria. *J Environ Radioact* 2005;79:119–25. doi: 10.1016/j.jenvrad.2004.05.016
47. Tufail M. Radium equivalent activity in the light of UNSCEAR report. *Environ Monit Assess* 2012;84:5663–7. doi: 10.1007/s10661-011-2370-6
48. Petrović M. *Potencijal ispiranja selen i metala iz nepropisno odloženog otpada šljake, pepela i Raškog ugljena u naselju Štrmac u Istri* [Leaching potential of selenium and metals from an unregulated waste of slag, ash and Raša coal (Štrmac, Istria), in Croatian]. [Master thesis]. Zagreb: University of Zagreb, Faculty of Science; 2019.
49. Petrović M. Selenium: widespread yet scarce, essential yet toxic. *Chem Texts* 2021;7:11. doi: 10.1007/s40828-021-00137-y
50. Halamić J, Miko S. *Geochemical Atlas of the Republic of Croatia*. Zagreb: Croatian Geological Survey; 2009.
51. *Pravilnik o zaštiti poljoprivrednog zemljišta od onečišćenja* [Ordinance on the protection of agricultural land from pollution, in Croatian]. *Narodne novine* 71/2019.

52. Reimann C, de Caritat P. *Chemical Elements in the Environment: Facts Heets for the Geochemist and Environmental Scientist*. Berlin, Heidelberg: Springer; 1998.
53. Koljonen T. *Geochemical atlas of Finland, Part 2: Till*. Geological Survey of Finland, Espoo 1992.
54. Kabata-Pendias A. *Trace Elements in Soils and Plants*. 4th ed. Boca Raton (FL): Taylor & Francis Group; 2010.
55. Cai C, Xiong B, Zhang Y, Li X, Nunes LM. Critical comparison of soil pollution indices for assessing contamination with toxic metals. *Water Air Soil Pollut* 2015;226:352. doi: 10.1007/s11270-015-2620-2
56. Kowalska BJ, Mazurek R, Gasiorek M, Zaleski T. Pollution indices as useful tools for the comprehensive evaluation of the degree of soil contamination – A review. *Environ Geochem Health* 2018;40:2395–420. doi: 10.1007/s10653-018-0106-z
57. Pravilnik o praćenju stanja radioaktivnosti u okolišu [Ordinance on environmental monitoring of radioactivity, in Croatian]. *Narodne novine* 40/2018; 6/2022.
58. Getaldić A, Surić Mihić M, Veinović Ž, Skoko B, Petrincec B. Remediation of coal ash and slag disposal site: Comparison of radiological risk assessment. *Rud Geol Naft Zb* 2023;3:99–104. doi: 10.17794/rgn.2023.3.8
59. Das D, Rout PK. A review of coal fly ash utilization to save the environment. *Water Air Soil Pollut* 2023;234:128. doi: 10.1007/s11270-023-06143-9
60. Labrincha J, Puertas F, Schroyers W, Kovler K, Pontikes Y, Nuccetelli C, Krivenko P, Kovalchuk O, Petropavlovsky O, Komljenovic M, Fidanchevski E, Wieggers R, Volceanov E, Gunay E, Sanjuán MA, Ducman V, Angjusheva B, Bajare D, Kovacs T, Bator G, Schreurs S, Aguiar J, Provis JL. NORM by-products to building materials. In: Schroyers W, editor. *Naturally occurring radioactive materials in construction*. Duxfort: Woodhead publishing – Elsevier; 2017. p. 183–252.
61. Shi Y, Jiang F, Wang R, Yang S, Zhu X, Shen Y. A mini review on the separation of Al, Fe and Ti elements from coal fly ash leachate. *Int J Coal Sci Technol* 2024;11:24. doi: 10.1007/s40789-024-00683-z

Karakterizacija tla i pepela analizom elemenata u tragovima i radionuklida s napuštenog odlagališta pepela povezanoga s nekadašnjom industrijom raškog ugljena

Sastav elemenata u tragovima i radionuklida na odlagalištu pepela i u tlu odražava aktivnosti izgaranja koje su se provodile u prošlosti na superorgansko-sumpornom (SHOS) raškom ugljenu u zapadnoj Hrvatskoj. Posljedice na okoliš od napuštenog odlagališta ugljena i pepela bit će dugotrajne te se tijekom tog razdoblja mogu osloboditi velike količine čestica ugljena i pepela u okoliš. Cilj ovog istraživanja bio je doprinijeti znanju o ovoj temi i istražiti potencijalni utjecaj na okolno tlo i lokalno stanovništvo. Za karakterizaciju lokacije, uzorci pepela i tla prikupljeni su tijekom dviju kampanja uzorkovanja. Elementi u tragovima istraženi su elementarnom analizom pomoću rendgenske emisije inducirane česticama (PIXE). Analize radionuklida provedene su visokorezolucijskom gama-spektrometrijom. Određeni su sljedeći prirodni radionuklidi: ^{232}Th , ^{238}U , ^{226}Ra , ^{210}Pb i ^{40}K . PIXE analiza pokazala se korisnom u karakterizaciji uzoraka onečišćenog tla iz Štrmca te je dala rezultate u skladu s prethodnim istraživanjima. Analize radionuklida pokazale su veće koncentracije aktivnosti ^{238}U , ^{226}Ra i ^{210}Pb u uzorcima pepela. Indeksi koji su se koristili za procjenu radioloških učinaka odlagališta na lokalno stanovništvo pokazali su vrijednosti više od preporučenih, a stope apsorbirane doze za lokalno stanovništvo bile su do četiri puta veće od vrijednosti pozadinskog zračenja. Rezultati ovog istraživanja upućuju na potrebu istraživanja starih lokacija u industriji ugljena, kao i na važnost sanacije takvih lokacija.

KLJUČNE RIJEČI: NORM; pepeo; PIXE; radionuklidi; raški ugljen; štetni elementi u tragovima; tlo